Cluster structure of ^{17}O

S. Yu. Mezhevych, A. T. Rudchik, A. A. Rudchik, and O. A. Ponkratenko
Institute for Nuclear Research, Ukrainian Academy of Sciences, Prospect Nauki 47, 03680 Kyiv, Ukraine

N. Keeley*
National Centre for Nuclear Research, ul. Andrzeja Sołtana 7, PL-05-400 Otwock, Poland

K. W. Kemper
Department of Physics, The Florida State University, Tallahassee, Florida 32306, USA

M. Mazzocco
Dipartimento di Fisica e Astronomia, Università di Padova, via F. Marzolo 8, I-35131 Padova, Italy and INFN-Sezione di Padova, via F. Marzolo 8, I-35131 Padova, Italy

K. Rusek
Heavy Ion Laboratory, University of Warsaw, Pasteura 5A, PL-02-093 Warsaw, Poland

S. B. Sakuta
Russian Research Center "Kurchatov Institute", 123182 Moscow, Russia
(Received 19 July 2016; revised manuscript received 14 February 2017; published 16 March 2017)

The transfer reaction ^{13}C(^{11}B ,^{7}Li)^{17}O leading to the ground and several excited states of ^{17}O was investigated at an incident boron beam energy of 45 MeV. The experimental data were analyzed by means of coupled-channel Born approximation calculations and $^{17}\mathrm{O} = \alpha + {}^{13}\mathrm{C}$ spectroscopic factors were extracted from a comparison of the data and the calculations at forward angles. The largest spectroscopic factor obtained was that for the subthreshold 6.356 MeV $1/2^+$ state, important for the production of neutrons in the stellar environment, and the squared Coulomb modified asymptotic normalization coefficient, $\tilde{C}^2$, is consistent with previous determinations. A significant rise in the experimental data at backward scattering angles suggested the possibility of $^{17}\mathrm{O} = {}^{6}\mathrm{Li} + {}^{11}\mathrm{B}$ clustering in some ^{17}O states, including the ground state. However, explicit inclusion of ^{6}Li transfer in the calculations could not explain the observed effect. Compound nucleus calculations suggested that while the backward angle rise could be explained by such processes for two of the populated ^{17}O states other multistep direct processes must contribute significantly to the other two.

DOI: 10.1103/PhysRevC.95.034607

I. INTRODUCTION

Early α-structure calculations by Kurath [1] showed that the (^{11}B, ^{7}Li) reaction might be a good means to explore α clustering in nuclei. Early work using the ^{12}C(^{11}B , ^{7}Li)^{16}O reaction by Barnà *et al.* [2] at a large number of bombarding energies showed that the spectroscopic strengths extracted from distorted-wave Born approximation (DWBA) calculations were consistent with those obtained from other α transfer reactions and were essentially energy independent. Recently, Guo *et al.* [3] explored the use of the ^{13}C(^{11}B , ^{7}Li)^{17}O reaction at a bombarding energy of 50 MeV to extract both the spectroscopic factor and the asymptotic normalization coefficient (ANC) for the subthreshold 6.356 MeV $1/2^+$ state in ^{17}O, known to be important for the production of neutrons in the stellar environment through the ^{13}C(α,n) reaction. Their work focused on the states in ^{17}O at 3.055 MeV ($1/2^-$), 3.843 MeV ($5/2^-$), 4.554 MeV ($3/2^-$), and 6.356 MeV ($1/2^+$), with the main emphasis on the latter state.

The present work reports new data for the ^{13}C(^{11}B , ^{7}Li)^{17}O reaction taken at a ^{11}B beam energy of 45 MeV. With the experimental setup employed it was possible to detect both the ^{7}Li and ^{17}O particles so that forward and backward angle scattering data were acquired simultaneously. In an extensive series of experiments between 1p-shell beams and targets that employ inverse kinematics to collect data for both scattering and reactions, it has been shown that in some cases the backward angle cross sections are much larger than expected and can be used to study the influence of breakup, single- and multiparticle transfer and other strong coupling effects. One of the goals of the present work was to determine the extent to which the exotic cluster ^{6}Li is present in ^{13}C and ^{17}O.

Coupled-channel Born approximation (CCBA) calculations were carried out to extract the α spectroscopic amplitudes for the ground and 0.87 MeV states as well as the states studied by Guo *et al.* [3]. The sensitivity of the extracted amplitudes to the various components required to carry out the CCBA calculations was extensively explored. Once the forward angle data were described, calculations were performed to determine whether the large angle cross section data could be described by ^{6}Li cluster transfer or if the magnitude of

*Corresponding author: nicholas.keeley@ncbj.gov.pl

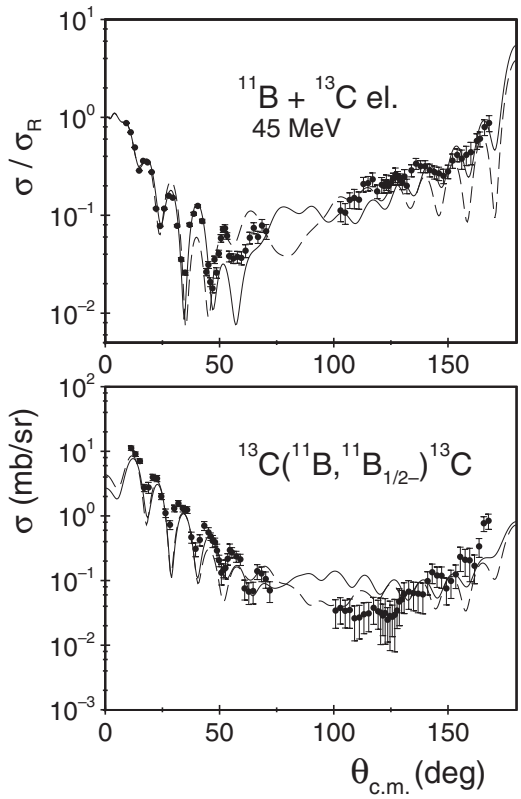

FIG. 1. Angular distributions of the elastic and inelastic scattering leading to the first excited state of ^{11}B. The curves denote the results of coupled-channel calculations with the optical potentials listed in Table 1 (solid: potential B, dashed: potential A). The experimental data are from Ref. [4].

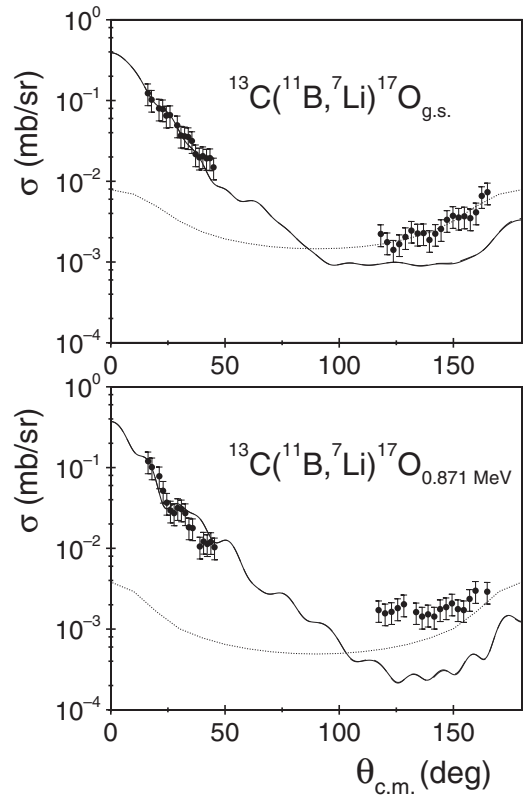

FIG. 2. Angular distributions of the emitted ^{7}Li and ^{17}O. The solid curves show the results of the CCBA α transfer calculations while the dashed curves (almost identical with the solid curves for these states) denote the sum of the α and ^{6}Li transfer results with the $S_{^6\mathrm{Li}}$ from Table II. The dotted curves denote the results of compound nucleus calculations with the code HELGA, see text for details.

the data showed that they could only be described by a mixture of complicated reaction processes. The present work demonstrates that extracting both forward angle and backward angle data can greatly enhance our understanding of reactions between complex nuclei.

II. EXPERIMENT

The experiment was performed at the Heavy Ion Laboratory of the University of Warsaw. A self-supporting carbon foil with 90% ^{13}C enrichment was used as a target. The reaction products were detected in ΔE-E telescopes, each consisting of a gas ionization chamber and a 1 mm thick silicon detector. Argon was used as the working gas. The energy loss of the ions in the ionization chamber corresponded to that deposited in an approximately 15 μm thick silicon detector. The detection system allowed for good separation of the isotopes produced in the ^{11}B +^{13}C interaction.

The elastic and inelastic scattering data plotted in Fig. 1 are taken from Ref. [4] where more information on the experimental setup may be found.

The experimental data for the ^{13}C(^{11}B , ^{7}Li)^{17}O transfer reaction are presented in Figs. 2–4. Angular distributions were measured at forward and backward angles (Figs. 2 and 3) for the reaction leading to the ^{17}O ground state and excited states at 0.871 MeV, 3.055 MeV, and 3.843 MeV while for the two higher ^{17}O excited states at 4.554 MeV and 6.356 MeV data at forward angles only were obtained (Fig. 4) since the recoil ^{17}O is unbound for these two states. The contribution to the yields from ^{12}C in the ^{13}C target was less than 10% based on the published cross sections of Ref. [4].

III. RESULTS

The transfer data were analyzed by means of CCBA calculations. Coupling to the first excited state of ^{11}B at 2.12 MeV was included in the calculations since it has been shown that this coupling has a considerable effect on the elastic scattering [5]. It was assumed that this state is a member of a $K = 1/2$ rotational band with a quadrupole deformation length $\delta_2 = 1.2$ fm [4]. The measured differential cross sections for the transfer channels were fairly small. A test coupled reaction channel calculation found the effect of these transfer channels on the elastic and inelastic scattering to be negligible, hence justifying the use of CCBA.

In the entrance channel, the optical model (OM) potential from the previous study [4] was adopted as the starting point, with a slightly reduced depth of the imaginary part (from 8 MeV to 7 MeV, Potential A in Table I). Keeley *et al.* [6] have shown that in a study of the ^{13}C(^{6}Li ,d)^{17}O reaction

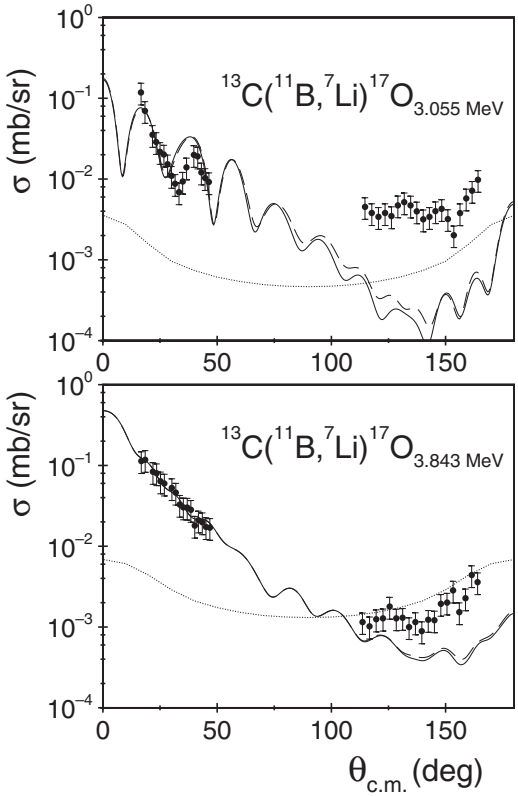

FIG. 3. As in Fig. 2 but for the 3.055 MeV and 3.843 MeV excited states of ^{17}O.

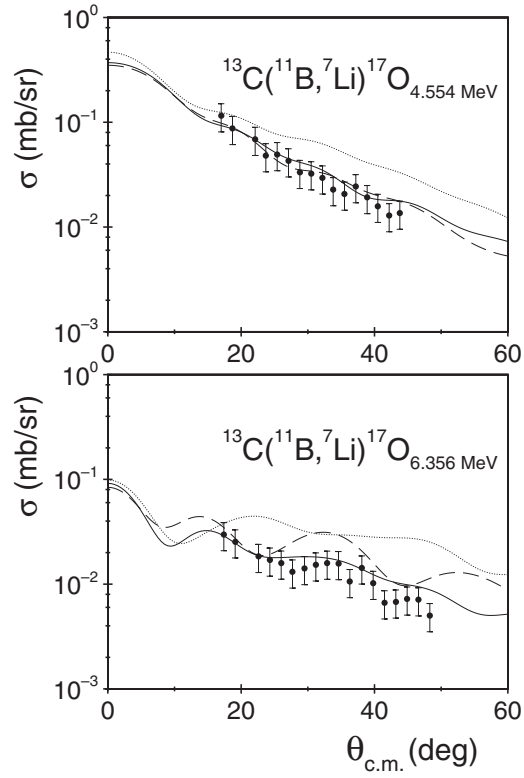

FIG. 4. Comparison of the experimental and theoretical results for the 4.554 MeV and 6.356 MeV excited states of ^{17}O. All the curves show the results of CCBA α transfer calculations: solid, as in Figs. 2 and 3; dashed, with Potential A in the entrance channel; dotted, with the global OM potential of Ref. [10] in the exit channel.

the values of the ^{17}O α spectroscopic factors extracted from a comparison of model calculations with the experimental data strongly depend on the choice of the entrance channel OM potential. Therefore, an automatic search was performed (coupled-channel calculations with coupling to the first excited state of ^{11}B included) on the entrance channel OM potential parameters in order to improve the fit to the elastic scattering data at forward angles. The searching version SFRESCO of the computer code FRESCO [7] was used for this purpose. The results are plotted as the solid curves in Fig. 1 and listed in Table I (Potential B). The overall description of the elastic scattering data with this potential was improved so it was therefore used in the transfer reaction data analysis.

The exit channel OM potential for the ^{7}Li + ^{17}O scattering system was determined earlier in Ref. [8] and successfully tested in a coupled reaction channel study of the one-neutron transfer reaction ^{18}O(^{6}Li ,^{7}Li)^{17}O [9].

A. α transfer

Potentials binding the transferred particle to the core are always important ingredients of transfer reaction calculations. In order to compare the results of this study with those published by Guo *et al.* [3] the same procedure for fixing the parameters of the $\alpha + {}^{7}$Li and $\alpha + {}^{13}$C binding potentials

TABLE I. Parameters of the Woods-Saxon potentials. Radii are defined according to the heavy-ion convention, $R = r_0(A_1^{1/3} + A_2^{1/3})$.

	V_0 MeV	r_0 fm	a_0 fm	W MeV	r_i fm	a_i	Ref.
^{11}B + ^{13}C Pot. A	256.7	0.788	0.740	7.00	1.250	0.740	[4]
^{11}B + ^{13}C Pot. B	220.5	0.927	0.617	24.36	0.523	1.271	this work
^{7}Li + ^{17}O	183.0	0.800	0.740	6.00	1.450	0.740	[8]
^{7}Li + ^{13}C	114.2	0.709	0.856	35.85	0.959	0.809	[10]
^{7}Li + ^{11}B	114.2	0.691	0.856	36.49	0.935	0.809	[10]
^{11}B$_{g.s.}$ = α + ^{7}Li	66.4	0.92	0.65	0.0	0.0	0.0	this work
^{17}O$_{g.s.}$ = α + ^{13}C	53.08	1.03	0.65	0.0	0.0	0.0	this work
^{17}O$_{g.s.}$ = ^{6}Li + ^{11}B	127.15	0.794	0.65	0.0	0.0	0.0	this work
^{13}C$_{g.s.}$ = ^{6}Li + ^{7}Li	145.24	0.788	0.65	0.0	0.0	0.0	this work

TABLE II. Spectroscopic amplitudes from the TISM used in the FRESCO calculations ($A = C + x$, where $x = \alpha$ or ^{6}Li). The number of nodes (N) in the radial wave function includes that at the origin but not that at infinity.

A	E_{ex} (MeV)	C	NL_J	S_x
^{17}O	0.00	^{13}C	$2F_3$	−0.191
		^{11}B	$2F_2$	0.255
			$2F_3$	−0.208
			$2F_4$	0.074
^{17}O*	0.871	^{13}C	$3P_1$	0.539
		^{11}B	$3P_1$	0.263
			$2F_2$	−0.162
^{17}O*	3.055	^{13}C	$4S_0$	−0.539
		^{11}B	$4S_1$	−0.263
			$3D_1$	−0.162
			$3D_2$	0.485
^{17}O*	3.843	^{13}C	$3D_2$	0.192
		^{11}B	$4S_1$	−0.623
			$3D_1$	−0.028
			$3D_2$	−0.095
			$3D_3$	−0.170
^{17}O*	4.554	^{13}C	$3D_2$	0.536
^{17}O*	6.356	^{13}C	$3P_1$	0.539
^{13}C	0.000	^{7}Li	$3S_1$	−0.124
			$2D_1$	−0.039
			$2D_2$	−0.116
^{11}B	0.000	^{7}Li	$3S_0$	−0.638
			$2D_2$	−0.422

was used, namely the potentials binding the α particle to the ^{7}Li and ^{13}C cores were of standard Woods-Saxon form, with diffuseness parameter $a = 0.65$ fm and radii obtained by folding the matter densities of the transferred particle and the core with their relative motion. This led to equation (1) of Ref. [3]. The radii of ^{7}Li , ^{11}B, and ^{13}C taken from Ref. [11], the radius of ^{17}O from Ref. [12] and the radius of ^{4}He (1.47 fm [3]) were used in this equation and the radii of the α binding potentials calculated. The parameters of the binding potentials are listed in Table I.

The interaction potential was calculated from the binding potentials, OM potentials in the entrance or exit channels (according as the *post* or *prior* form was used) and the core-core (^{7}Li +^{13}C) OM potential listed in Table I. The results of the CCBA calculations were almost identical for both forms (*post* and *prior*). Those plotted in Figs. 2–4 were obtained using the *post* form of the interaction potential.

The results of the calculations depend on the product of two spectroscopic factors: that for the projectile (^{11}B) and that for the final nucleus (^{17}O). The spectroscopic factors are the squares of the spectroscopic amplitudes. The amplitudes for the ^{17}O states were calculated using the translationally invariant shell model (TISM) [13,14] and are listed in Table II. They were used as a starting point in the CCBA calculations performed using the code FRESCO [7]. Spectroscopic amplitudes calculated with the TISM were also used for ^{11}B. They are slightly different from those calculated previously by Kurath [1], but as was shown in Ref. [3] and tested in this work,

TABLE III. α spectroscopic factors (S^2_α) of ^{17}O states from α transfer experiments and the TISM. The Ref. [6] values were taken from the "CRC (2p-1h)" column of Table 3.

E_{ex}	I^π	this work	Ref. [3]	Ref. [15]	Ref. [6]	TISM
0.000	$5/2^+$	0.08 ± 0.02			0.12	0.036
0.871	$1/2^+$	0.35 ± 0.12			0.17	0.29
3.055	$1/2^-$	0.42 ± 0.16	0.19 ± 0.06	0.27 ± 0.05	0.30	0.29
3.843	$5/2^-$	0.10 ± 0.03	0.078 ± 0.025		0.34	0.037
4.554	$3/2^-$	0.15 ± 0.05	0.06 ± 0.09	0.10 ± 0.05	0.49	0.29
6.356	$1/2^+$	0.39 ± 0.12	0.37 ± 0.12	0.29 ± 0.11	0.40	
6.356	$1/2^+$	0.72 ± 0.22[a]				0.29[a]

[a] $N = 3$.

the results of the model calculations are very similar with these two sets of amplitudes, provided that the signs of the Kurath amplitudes are taken to be the same as those obtained from the TISM calculations.

The calculations were normalized to the data at the most forward angles and such normalized results are given by the solid curves in Figs. 2–4. The spectroscopic factors (squares of the spectroscopic amplitudes) corresponding to this normalization are listed in Table III. The errors listed in Table III correspond to the statistical errors on the measured differential cross sections. The spectroscopic amplitudes for ^{11}B were not changed in the calculations and kept equal to those listed in Table II. Comparison of absolute spectroscopic factors obtained in different studies is always problematical due to the dependence of these quantities on the parameters of the binding potentials used, in addition to the question of whether the reaction mechanism has been modeled adequately. However, the uncertainties on the values given in Refs. [3] and [15] take into account the effect of employing a range of bound state radius and diffuseness parameters which covers the values used in this work. Therefore we should see agreement between all three evaluations within the stated uncertainties. The comparison with the spectroscopic factors of Ref. [6] is admittedly more problematic since the bound state radius used is somewhat larger.

The smallest values were obtained for the ground state and the 3.843 MeV state of ^{17}O, in qualitative agreement with the TISM predictions and in quantitative agreement with Ref. [3] for the 3.843 MeV state. The value for the first excited state is in agreement with the TISM calculation, as is the value for the 3.055 MeV state which in addition is in agreement with the results of two previous α transfer studies [6,15]. For the 4.554 MeV state the value obtained is in agreement with those of Refs. [3,15] and close to the TISM but very different from that of Ref. [6]. The three previous α transfer studies listed in Table III (Refs. [3,6,15]) gave very similar results for the important $1/2^+$, 6.356 MeV state, while the value of the spectroscopic factor obtained in this work is much larger. This is due to the smaller number of nodes in the radial wave function used here ($N = 3$ as compared to $N = 4$ in Refs. [3,6,15]) following the predictions of the TISM calculations; if $N = 4$ is used our analysis yields a value of $S^2_\alpha = 0.39 \pm 0.12$ for this state, in excellent agreement with the previous determinations. However, these spectroscopic factors correspond to values

for the squared Coulomb modified ANC of $\tilde{C}^2 = 5.1 \pm 1.5$ fm^{-1} and $\tilde{C}^2 = 4.5 \pm 1.4$ fm^{-1} for $N = 3$ and $N = 4$, respectively, in good agreement with the results of Refs. [3] (4.0 ± 1.1), [15] (4.5 ± 2.2), and [16] (3.6 ± 0.7). Thus $\tilde{C}^2$ is relatively insensitive to the choice of N, as found by Pellegriti *et al.* [15].

Agreement between the spectroscopic factors obtained in this work and those of Refs. [3] and [15] is good (if we compare the present result for the 6.356 MeV $1/2^+$ state obtained with $N = 4$) while that with Ref. [6] is rather less so, which may be explained, at least in part, by the somewhat different binding potential parameters used in that work. The present empirical spectroscopic factors are in quantitative agreement with the TISM results for the 0.871 MeV $1/2^+$ and 3.055 MeV $1/2^-$ states only, the values for the other states only agreeing to within a factor of 2 or so. However, as has been known for a long time, the absolute values of α-particle transfer reaction calculations can be very sensitive to the distorting potentials used. A series of test calculations was performed in order to establish the sensitivity of the calculated results to these parameters and determine whether this could account for the discrepancies between the empirical and TISM spectroscopic factors. The results are plotted in Fig. 4. The dependence on the entrance channel OM potential parameters may be seen by comparing the solid and dashed curves (Potentials A and B, respectively). The choice of entrance channel OM potential does not greatly affect the results of the CCBA calculations at forward angles, although for the 6.356 MeV state a significant effect is already noticeable at about 10°. If, instead of the empirical ^{7}Li OM potential for the exit channel obtained in Ref. [8] the global ^{7}Li $+A$ OM potential of Ref. [10] was used, the results of the CCBA calculations were similar only at very forward angles (solid and dotted curves, respectively). In the angular range where we have data the calculations with the OM potential of Ref. [10] in the exit channel both overpredict the magnitude of the cross section. The shape is also not as well reproduced, the dotted curves falling too slowly with angle compared to the data. The choice of distorting potentials in entrance and/or exit channels would therefore not appear to be able consistently to account for the discrepancies between the empirical and TISM S_α^2 values, the most likely explanation being that the structure of at least some of these ^{17}O states is more complicated than was assumed in the TISM calculations.

B. ^{6}Li transfer

A major effort of this work was to measure the angular distributions of the reaction products for the four transfer channels leading to the ground state, 0.871 MeV, 3.055 MeV, and 3.843 MeV states of ^{17}O at forward and backward angles to determine whether α spectroscopic strengths would be better determined by fitting data over the complete angular range. The fact that CCBA calculations including just α transfer were not able to account for the rise in the differential cross section at backward angles (Figs. 2 and 3) led to the search for other transfer mechanisms, one of the most obvious being transfer of a ^{6}Li cluster from the target to the projectile since the TISM calculations predict sizable spectroscopic amplitudes for the $^{13}\mathrm{C} = {}^7\mathrm{Li} + {}^6\mathrm{Li}$ and $^{17}\mathrm{O} = {}^6\mathrm{Li} + {}^{11}\mathrm{B}$ cluster structures (Table II). Thus, CCBA calculations for ^{6}Li transfer were performed in order to investigate the contribution of this mechanism to the observed rise of the large angle cross sections.

For such a large cluster, the method for estimating the radii of the cluster binding potentials used in the previous section could not be applied since the radius of ^{6}Li is much larger than that of the α particle and even larger than that of ^{13}C [11]. Therefore, the radii of the ^{6}Li binding potentials in ^{13}C and ^{17}O were set to the "standard" radii of these nuclei, $R_{^{13}\mathrm{C}} = 1.25 \times 13^{1/3}$ fm and $R_{^{17}\mathrm{O}} = 1.25 \times 17^{1/3}$ fm. The potentials were of Woods-Saxon form, with a diffuseness of 0.65 fm and the depth adjusted to give the correct binding energy for these systems. The parameters are listed in Table I.

Calculations using the spectroscopic amplitudes from the TISM (Table II) gave results that were essentially identical to those obtained without including ^{6}Li transfer. Only in the case of transfer to the 3.055 MeV and (barely) the 3.843 MeV states of ^{17}O is the effect visible at backward angles, see the dashed curves in Figs. 2 and 3 which represent the coherent sums of the α and ^{6}Li transfers. It is therefore readily apparent that ^{6}Li transfer cannot be responsible for the observed rise in the differential cross section at backward angles, even allowing for the uncertainties in the calculations.

C. Compound nucleus calculations

Another possible explanation for the observed backward angle rise in the transfer angular distributions is the presence of a significant compound nucleus component. However, as is apparent from a comparison of Figs. 2 and 3, the backward angle cross sections do not scale with $(2J + 1)$, as required by the statistical model, cf. the backward angle cross sections for transfer to the 0.871 MeV excited state of ^{17}O ($1/2^+$) which are about a factor of two smaller than those for transfer leading to the 3.055 MeV state ($1/2^-$). Also, the backward angle cross sections for the 3.055 MeV ($1/2^-$) state are considerably larger than those for the 0.0 MeV ($5/2^+$) state whereas the reverse should be true for a statistical compound nucleus mechanism. This strongly suggests that the large angle cross sections measured in this work for the ^{17}O+^{7}Li exit channel cannot be fully explained by evaporation from the compound nucleus ^{24}Na either.

However, to explore further this possibility, compound nucleus calculations were carried out with the computer code HELGA [17]. Calculations for the compound process were explored in great detail in the mid and late 1970s in the hope of using this reaction process to assign final state spins for nuclei like ^{20}Ne produced in the reactions ^{12}C(^{14}N,^{6}Li)^{20}Ne and ^{10}B(^{12}C,d)^{20}Ne. It was assumed that the final states observed were populated through the compound process and these data provided a way to explore the sensitivity of the calculated absolute cross section to the various input parameters. An important observation was the need to use a critical angular momentum in calculating absolute cross sections [18], which could be derived from measured fusion cross sections if one assumed a sharp cutoff approximation for the transmission coefficients (see Eq. 2 of Ref. [19]). The sensitivity to input parameters, such as the continuum level density, optical

potentials, and critical angular momenta, required for determining the absolute cross section, was thoroughly investigated. For example, changing the level density parameter by 20% was found to change the cross section by a factor of 6. Similar results were found for different sets of optical potentials as well as slight changes in the critical angular momentum. However, it was found that the relative cross sections between partitions and between the states in a given partition were quite robust and not subject to the wide variations observed as a function of the input parameters for the absolute cross section.

The practical solution that was adopted is the one used here, and that is to take a channel, usually one with the smallest cross section or one that might not be a direct one-step transfer such as ^{12}C(^{6}Li ,d)^{16}O (8.87 2$^-$) and make slight adjustments to the critical angular momentum derived from the sharp cutoff approximation to the fusion cross section until the desired cross section is produced. A survey of fusion cross sections for systems in this mass region as well as the result of assuming that 90% of the total reaction cross section calculated with the optical potential parameters used as input to HELGA was due to fusion gave a total fusion cross section of 1000 mb from which an angular momentum cutoff for this system of 11.5$\hbar$ was extracted [19]. The cutoff angular momentum was then decreased from 11.5$\hbar$ to 11$\hbar$ to match the measured cross section for the 0.0 MeV $5/2^+$ state in ^{17}O. The compound nucleus cross sections obtained for the other three states populated in the ^{17}O+^{7}Li partition are presented in Figs. 2 and 3 (the compound nucleus contributions to the ^{13}C+^{11}B elastic scattering and inelastic scattering to the ^{11}B first excited state are negligible). It is apparent from Figs. 2 and 3 that the procedure adopted enables an excellent description of the shape of the backward angle data for population of the $5/2^+$ ground state of ^{17}O by the compound nucleus process—the calculations were arranged so that the magnitude was reproduced—and a satisfactory description of the backward angle data for population of the 3.843 MeV $5/2^-$ state (the shape is well reproduced but the magnitude is slightly overpredicted). However, the backward angle data for population of the 0.871 MeV $1/2^+$ and 3.055 MeV $1/2^-$ states are not well reproduced, either with regard to the magnitude which is significantly underpredicted in both cases, particularly so for the $1/2^-$ state, or the shape, the experimental data having much "flatter" angular distributions than the compound nucleus calculations. The calculations therefore suggest that while compound nucleus processes could account for essentially all the observed backward angle rise in the angular distributions for populating the two spin-5/2 states in ^{17}O they can only partially account for this phenomenon for the two spin-1/2 states. In particular, the backward angle rise in the 3.055 MeV $1/2^-$ state data must be due predominantly to other processes, presumably multistep direct transfer(s) of some sort.

IV. SUMMARY

Angular distributions of the ^{13}C(^{11}B ,^{7}Li)^{17}O transfer reaction leading to six states of the final nucleus were measured. The data were analyzed by means of CCBA calculations that included coupling to the first excited state of the projectile nucleus. The α spectroscopic factors of the ^{17}O states were determined from a comparison of the CCBA calculations and the experimental data at the most forward angles. Good agreement was obtained with previous determinations [3,15]. The largest value was for the subthreshold $1/2^+$ state at an excitation energy of 6.356 MeV, either $S_\alpha^2 = 0.72 \pm 0.22$ or $S_\alpha^2 = 0.39 \pm 0.12$, depending on whether the number of nodes in the radial wave function was as predicted by the TISM ($N = 3$) or as used in previous determinations [3,15] ($N = 4$), respectively. The $N = 4$ result is in good agreement with previous determinations [3,6,15] but the $N = 3$ result is approximately a factor of 2 larger than the TISM prediction. However, the Coulomb modified ANCs for both values of N, $\tilde{C}^2 = 5.1 \pm 1.5$ fm^{-1} ($N = 3$) and $\tilde{C}^2 = 4.5 \pm 1.4$ fm^{-1} ($N = 4$), are in good agreement with the values obtained in Refs. [3,15,16] and are essentially independent of the choice of N.

The present work complements a previous study of the same reaction at a very similar energy [3] by measurements of the angular distributions at backward angles. The rise in the differential cross section at backward angles suggested the possibility of an "exotic" clustering mode, ^{6}Li +^{11}B, for the $5/2^+$ ground state, $1/2^+$ 0.871 MeV, $1/2^-$ 3.055 MeV, and $5/2^-$ 3.843 MeV states of ^{17}O. However, explicit inclusion of ^{6}Li transfer could not explain the observed effect. Compound nucleus calculations with the code HELGA, normalized to describe the backward angle data for population of the $5/2^+$ ground state of ^{17}O, could only partially account for the observed rise in the backward angle differential cross sections for populating the other states. In particular, the cross sections for the two spin-1/2 states were significantly underpredicted by the compound nucleus calculations, suggesting that other multistep direct processes are important in the population of these states at least.

ACKNOWLEDGMENTS

This work was partially supported by the National Science Centre of Poland under Contract No. UMO-2014/14/M/ST2/00738 (COPIN-INFN Collaboration). K.W.K. acknowledges partial support from the Florida State University Robert O. Lawton Fund and would like to thank the staff of the Heavy Ion Laboratory of the University of Warsaw for hospitality during the period in which this work was carried out. The authors would like to thank Dr. D. D. Caussyn for his invaluable help in updating the HELGA code to run on currently available platforms.

[1] D. Kurath, Phys. Rev. C **7**, 1390 (1973).

[2] R. Barnà, V. D'Amico, D. De Pasquale, A. Italiano, A. Lamberto, L. Jarczyk, B. Kamys, M. Kistryn, A. Kozela, A. Magiera, Z. Rudy, A. Strzał kowski, S. Albergo, R. Potenza, and J. Romański, Phys. Rev. C **50**, 300 (1994).

[3] B. Guo, Z. H. Li, M. Lugaro, J. Buntain, D. Y. Pang, Y. J. Li, J. Su, S. Q. Yan, X. X. Bai, Y. S. Chen, Q. W. Fan, S. J. Jin, A. I. Karakas, E. T. Li, Z. C. Li, G. Lian, J. C. Liu, X. Liu, J. R. Shi, N. C. Shu, B. X. Wang, Y. B. Wang, S. Zeng, and W. P. Liu, Astrophys. J. **756**, 193 (2012).

[4] S. Yu. Mezhevych, K. Rusek, A. T. Rudchik, A. Budzanowski, V. K. Chernievsky, B. Czech, J. Choiński, L. Gł owacka, S. Kliczewski, E. I. Koshchy, V. M. Kyryanchuk, A. V. Mokhnach, A. A. Rudchik, S. B. Sakuta, R. Siudak, I. Skwirczyńska, A. Szczurek, and L. Zemło, Nucl. Phys. A **724**, 29 (2003).
[5] S. Yu. Mezhevych, Ph.D. thesis, The Andrzej Sołtan Institute for Nuclear Studies, 2005.
[6] N. Keeley, K. W. Kemper, and Dao T. Khoa, Nucl. Phys. A **726**, 159 (2003).
[7] I. J. Thompson, Comput. Phys. Rep. **7**, 167 (1988).
[8] A. T. Rudchik, K. A. Chercas, K. W. Kemper, A. A. Rudchik, S. Kliczewski, E. I. Koshchy, K. Rusek, S. Yu. Mezhevych, O. A. Ponkratenko, Val. M. Pirnak, V. A. Plujko, J. Choiński, B. Czech, R. Siudak, and A. Szczurek, Nucl. Phys. A **927**, 209 (2014).
[9] K. Rusek, N. Keeley, K. W. Kemper, and A. T. Rudchik, Phys. Rev. C **91**, 044612 (2015).
[10] J. Cook, Nucl. Phys. A **388**, 153 (1982).
[11] E. Liatard, J. F. Bruandet, F. Glasser, S. Kox, Tsan Ung Chan, G. J. Costa, C. Heitz, Y. El Masri, F. Hanappe, R. Bimbot, D. Guillemaud-Mueller, and A. C. Mueller, Europhys. Lett. **13**, 401 (1990).
[12] Hu-Yong Zhang, Wen-Qing Shen, Zhong-Zhou Ren, Yu-Gang Ma, Jin-Gen Chen, Xiang-Zhou Cai, Zhao-Hui Lu, Chen Zhong, Wei Guo, Yi-Bin Wei, Xing-Fei Zhou, Guo-Liang Ma, and Kun Wang, Chin. Phys. Lett. **20**, 1462 (2003).
[13] Yu. F. Smirnov and Yu. M. Tchuvilsky, Phys. Rev. C **15**, 84 (1977).
[14] A. T. Rudchik and Yu. M. Tchuvilsky, code DESNA, Report No. KIYAI-82-12, Kiev Institute of Nuclear Research (1982).
[15] M. G. Pellegriti, F. Hammache, P. Roussel, L. Audouin, D. Beaumel, P. Descouvemont, S. Fortier, L. Gaudefroy, J. Kiener, A. Lefebvre-Schuhl, M. Stanoiu, V. Tatischeff, and M. Vilmay, Phys. Rev. C **77**, 042801(R) (2008).
[16] M. L. Avila, G. V. Rogachev, E. Koshchiy, L. T. Baby, J. Belarge, K. W. Kemper, A. N. Kuchera, and D. Santiago-Gonzalez, Phys. Rev. C **91**, 048801 (2015).
[17] S. K. Penny, code HELGA (unpublished).
[18] H. V. Klapdor, H. Reiss, and G. Rosner, Nucl. Phys. A **262**, 157 (1976).
[19] L. C. Dennis, A. Roy, A. D. Frawley, and K. W. Kemper, Nucl. Phys. A **359**, 455 (1981).